JACS
JOURNAL OF THE AMERICAN CHEMICAL SOCIETY
Communication
Cite This: J. Am. Chem. Soc. 2018, 140, 118−121
pubs.acs.org/JACS

Self-Assembly of Chiral Metal−Organic Tetartoid

Dong Luo,[†,⊥] Xue-Zhi Wang,[‡,⊥] Chen Yang,[§] Xiao-Ping Zhou,*[,‡] and Dan Li*[,†]

[†]College of Chemistry and Materials Science, Jinan University, Guangzhou 510632, P. R. China
[‡]Department of Chemistry, Shantou University, Guangdong 515063, P. R. China
[§]Department of Chemistry and State Key Laboratory of Synthetic Chemistry, The University of Hong Kong, Pokfulam Road, Hong Kong, P. R. China

Supporting Information

ABSTRACT: Chiral coordination cages feature both chirality and defined inner space, providing advanced molecular materials. A series of chiral 20-nucleus cobalt-imidazolate cages were synthesized by self-assembly of 72 subcomponents, featuring a novel tetartoid (tetragonal pentagonal dodecahedron) structure. Spontaneous resolution of racemic tetartoidal cages (Δ and Λ) into a conglomerate of homochiral crystals are observed, while both homochiral Δ and Λ tetartoidal cages can be obtained through chiral induction of (D)- and (L)-enantiomers of menthol, respectively. The 2-methyl substituent on imidazolyl is critical to the formation of a tetartoidal cage, and the absence of such steric effect will switch the final structure to a cubic cage.

Self-assembly is an essential feature of supramolecular chemistry and plays a vital role in the creation of various biological systems (e.g., viruses).[1] Coordination-directed self-assembly toward well-defined metal−organic cages (or coordination cages) gives an elegant approach to mimic biologic self-assembly behavior.[2] Gigantic number of coordination cages based on Platonic and Archimedean solids and other nonclassical architectures have been successfully designed and synthesized by assembly of metal ions and organic ligands,[3] which show advanced functions in separation,[4] catalysis,[5] stabilization of reactive species,[6] drug delivery,[7] etc.

Although huge success has been made in the field of coordination cage, the structures assembled from a large number of components are difficult to forecast. Subtle differences in the ligands or reacting conditions may lead to distinct coordination cages. Fujita et al. showed that slight changes in bending angles of ligands and introduction of steric effect through a methyl group give rise to $M_{12}L_{24}$, $M_{24}L_{48}$, and $M_{30}L_{60}$ cages,[2b,8] and variation of crystal growth temperature induced the formation of an unusual $M_{48}L_{96}$ Goldberg polyhedron.[2b] Nitschke et al. reported perfluorinated ligands induced meridional metal stereochemistry to form M_8L_{12}, $M_{10}L_{15}$, and $M_{12}L_{18}$ prisms, while facial coordination yielded tetrahedral cages in the subcomponent self-assembly.[9] In our previous study, we found that changes of substituents of imidazole ligand or anion switched the final structure (cubic $Ni_8L_{12}X_4$ versus rhombic dodecahedral $Ni_{14}L_{24}$ cage).[10] So far, the understanding of rules of self-assembly via tuning subtle factor remains critical for designing targeted coordination cages.

Chirality is a fundamental property for chemistry and biology. Coordination cages can combine chirality and nanoscale cavity in an artificial molecule, giving rise to advanced applications such as enantioselective separation,[11] asymmetric catalysis,[12] and sensor[11a] for enantiomer. Two main approaches have been employed to synthesize chiral coordination cages: use of homochiral organic components and spontaneous resolution of chiral cage from achiral components through crystallization.[13] The former approach is mostly used for generating a homochiral coordination cage, whereas homochiral cages can also be obtained through the later approach because inherent chirality can arise via spatial organization of achiral components.[14] However, such resulting cages tend to form racemic crystals or racemic conglomerates of homochiral crystals in the absence of chiral additive.

Herein, we report the subcomponent self-assembly of a series of emerging polyhedral metal−imidazolate cages (Scheme 1),

Scheme 1. Subcomponent Self-Assembly of Metal Imidazolate Tetartoids and Cubes

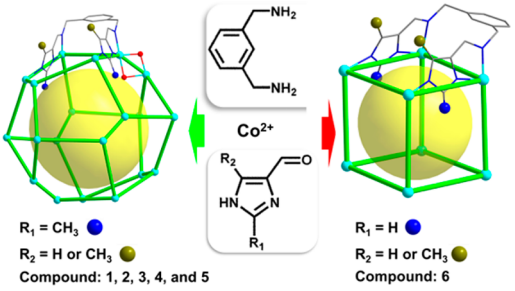

formulated as $[Co_{20}L_{12}(OH)_{12}(H_2O)_4]\cdot 8BF_4^-\cdot\chi$guest (**1** H_2L1 = 1,3-bis[(2-methyl-1*H*-imidazol-4-yl)methyleneaminomethyl]-benzene and **2** H_2L2 = 1,3-bis[(2,5-dimethyl-1*H*-imidazol-4-yl)methyleneaminomethyl]benzene). Cages **1** and **2** resulting from the self-assembly involving 72 components feature an unusual tetartoid (tetragonal pentagonal dodecahedron) geometry. Notably, both **1** and **2** are chiral with a *T* symmetry, which is identical with that of a tetrartoid. Spontaneous resolution of racemic tetartoidal cage into a conglomerate of homochiral crystals are confirmed by both single X-ray diffraction (SCXRD) analyses and solid-state circular dichroism (CD) spectra. Additionally, enantiomerically pure ΔΔΔΔ-**1** and ΛΛΛΛ-**1**

Received: October 23, 2017
Published: December 13, 2017

DOI: 10.1021/jacs.7b11285
J. Am. Chem. Soc. 2018, 140, 118−121

can be obtained by homochiral crystallization through chiral induction of (D)- and (L)-enantiomers of menthol, respectively. The 2-methyl group on the imidazolyl plays a structure-direct role for forming the tetartoidal cages, while cubic cages are obtained in the absence of steric effect of the 2-methyl group (Scheme 1).

Previously, we utilized subcomponent self-assembly[15] to synthesize a series of metal−imidazolate cages.[10,16] Here, the single crystals of **1** and **2** can be obtained through solvothermal subcomponent self-assembly (see the Supporting Information for details). SCXRD analysis revealed both **1** and **2** crystallized in cubic chiral space group *F*23 and feature 20-nucleus polyhedral structure (Figure 1). Only the structure of **1** will be described here. Both homochiral crystals of ΔΔΔΔ-**1** and ΛΛΛΛ-**1** are founded in one sample batch, forming a conglomerate.

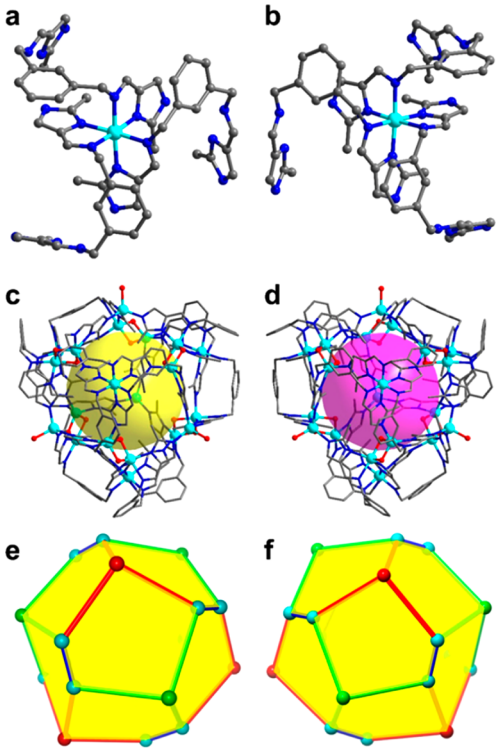

Figure 1. Crystal structures of two enantiomers of **1**: facial coordination in Δ (a) and Λ (b) absolute configuration for octahedral cobalt centers, the 20-nuclear chiral ΔΔΔΔ-**1** (c) and ΛΛΛΛ-**1** (d) cage-structures (yellow and purple large spheres represent the cavities in the cages), and simplified geometry of the obtained structure of ΔΔΔΔ-**1** (e) and ΛΛΛΛ-**1** (f). Each vertex represents a cobalt ion center, and each edge represents an imidazolate group (red and green stick) or OH^- group (blue stick), respectively. Color codes: Co, cyan; O, red; C, gray; N, blue; H, omitted.

Cage **1** contains three types of geometrically independent cobalt centers (octahedral, tetrahedral, and distorted square pyramidal). The octahedral cobalt center is chelated by three L1 and adopts a facial coordination with Δ and Λ absolute configuration in ΔΔΔΔ-**1** and ΛΛΛΛ-**1** (Figure 1a,b), respectively. The Co−N bond lengths range from 1.946 to 1.986 Å, indicating +3 valence. The tetrahedral cobalt center binds with three imidazolyl groups (Co−N = 2.001 Å) and one water, while the distorted square pyramidal cobalt center coordinates with three N and two O atoms (OH^-) with longer Co−N bonds (2.043 to 2.185 Å). Twelve L1 and 12 OH^- anions bridge four octahedral Co(III), four tetrahedral Co(II), and 12 distorted square pyramidal Co(II) to construct the unusual 20-nucleus nanoscale polyhedron, which has three types of edges with the length of 6.087, 6.187, and 3.077 Å (adjacent Co···Co distances), respectively. The Co···Co distance between two opposite octahedral Co(III) centers is 15.964 Å. Note that L1 is *in situ* synthesized from two formylimidazole and one *m*-xylylenediamine, and thus, cage **1** involves 72 subcomponents, which is the largest number of components among all artificial molecules obtained by subcomponent self-assembly.

The regular dodecahedron (I_h point group), the second largest Platonic solid, consists of 12 regular pentagonal faces, 20 vertexes, and 30 edges. It is more difficult to synthesize dodecahedral metal−organic cages, compared with those smaller Platonic bodies (tetrahedron, cube, and octahedron), due to its high symmetry and largest number of vertexes. Except for regular dodecahedron, there exist three lower symmetric dodecahedra with pentagonal faces, i.e., pyritohedron (T_h), tetartoid (T), and dual of triangular gyrobianticupola (D_{3d}) (Figure S2). The 20-nucleus cage **1** can be considered a tetartoid (Figure 1e,f) because (i) the 12 pentagonal faces in **1** are irregular and the cage symmetry is T; (ii) cage **1** contains three types of cobalt centers (4 + 4 + 12); (iii) cage **1** contains three types of linkers (6 + 12 + 12); (iv) cage **1** is chiral. All these features agree with that of a tetartoid. Interestingly, the mineral cobaltite (Figure S3, a sulfide mineral composed of cobalt, arsenic, and sulfur) also shows a tetartoidal form. To the best of our knowledge, **1** and **2** are the first artificial tetartoidal molecules discovered.

Cage **1** is slightly soluble in polar organic solvents such as *N*,*N*-dimethylacetamide (DMA) and acetonitrile at 65 °C. To confirm the formation of 20-nucleus cage **1** in solution, electrospray ionization-time-of-flight (ESI-TOF) mass spectrum in acetonitrile was measured. A sequence of cationic peaks arising from the consecutive loss of BF_4^- anions from **1** is observed (Figure 2). The main peaks corresponding to $\{[Co_{20}L1_{12}(OH)_{12}(H_2O)_w(CH_3CN)_x]\cdot nBF_4\cdot yH_2O\cdot zMeOH\}^{(8-n)+}$ (n = 3, 4, 5; w = 0−4, x = 0−4, y = 0−4, z = 0−7) are complicated; at least 26 peaks for $\{[Co_{20}L1_{12}(OH)_{12}(H_2O)_w(CH_3CN)_x]\cdot 4BF_4\cdot yH_2O\cdot zMeOH\}^{4+}$ species (Figure 2b) are observed. The 26 species have been identified by carefully comparing the experimented isotope distributions and the simulated patterns (insets of Figures 2b and S5−S8). The large number of species found in the mass spectra are probably ascribed to two reasons: (i) the water molecules binding to the tetrahedral cobalt centers were lost or replaced by acetonitrile molecules in the process of ionization and dissolution; (ii) the narrow pentagonal windows prevented the guest molecules (water and methanol) from entering or leaving the cavity of **1** freely (Figure S11). This carceplex behavior is similar to our reported $Ni_{14}L_{24}$ cage,[16a] which can act as carcerand to imprison guest molecules such as methylamine and methanol randomly.

To confirm the formation of conglomerate, six large single crystals of **1** were picked out (Figure S12) in one batch to test their chiral configuration by SCXRD and CD spectroscopy. As shown in Table S7, SCXRD analysis revealed that three crystals are ΔΔΔΔ-**1**, and the other three are ΛΛΛΛ-**1**. All Flack parameters of the six crystals are close to zero (Table S7), determining their absolute structures of Δ or Λ configuration. Solid-state CD spectra (Figure S13) showed the ΔΔΔΔ-**1** crystals gave negative Cotton effect located on 345 nm, while ΛΛΛΛ-**1** corresponded to positive Cotton effect. The consistent results of SCXRD and CD spectra undoubtedly prove the conglomerate formation.

To obtain homochiral cage ΔΔΔΔ-**1** or ΛΛΛΛ-**1**, we employed organic chiral additives to induce the formation of

DOI: 10.1021/jacs.7b11285
J. Am. Chem. Soc. 2018, 140, 118−121

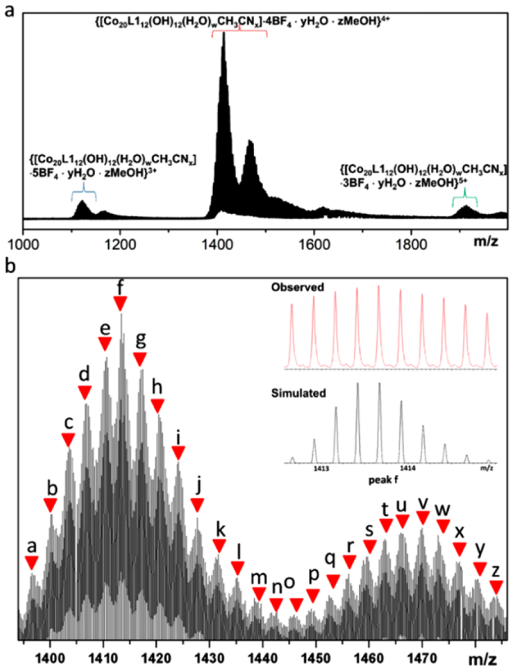

Figure 2. (a) ESI-TOF mass spectrum of **1**. (b) Expanded spectra for 26 species of $\{[Co_{20}L1_{12}(OH)_{12}(H_2O)_w(CH_3CN)_x]\cdot 4BF_4\cdot yH_2O\cdot zMeOH\}^{4+}$ (peaks *a*–*z*: $w = 0$–4, $x = 0$–4, $y = 0$–4, $z = 0$–7). Insets show the observed and simulated isotopic patterns of the peaks at m/z 1413.6613 (peak f) corresponding to the species of $\{[Co_{20}L1_{12}(OH)_{12}(H_2O)_4]\cdot 4BF_4\cdot MeOH\}^{4+}$.

enantiopure products.[17] Homochiral (D)- and (L)-menthol are chosen due to the multichiral centers and OH groups, which may interact with the tetartoidal cage through hydrogen bonds. Both enantiopure crystals of **ΔΔΔΔ-1** and **ΛΛΛΛ-1** were successfully obtained with the addition of (D)- and (L)-menthol into reactants, respectively (see Supporting Information). The PXRD patterns of **ΔΔΔΔ-1** and **ΛΛΛΛ-1** are identical with the simulated pattern for **1** (Figure S14). Solid-state CD spectra revealed bulk samples exhibited similar Cotton effects with that of single crystal **ΔΔΔΔ-1** and **ΛΛΛΛ-1** (Figure S13), but showing enhanced chiral signal (Figure 3). There was no CD signal in the absence of

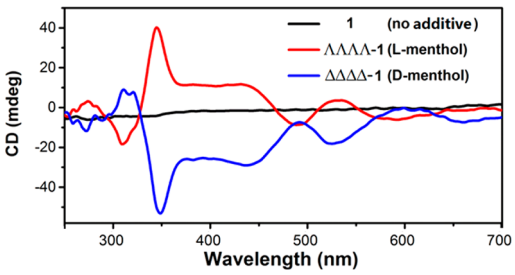

Figure 3. Solid-state CD (top) spectra of bulk samples obtained in the presence or absence of (D)- and (L)-menthol.

chiral additive, suggesting the presence of chiral menthol is critical for formation of homochiral bulk samples. Five sets of parallel experiments of chiral induction were performed (Figure S15), with only one set being ineffective, indicating the probability of obtaining enantiomeric excess product is ca. 80% when enantiopure menthol is used.

To further examine the influence of anions, we used ClO_4^-, PF_6^-, and $CF_3SO_3^-$ instead of BF_4^-. Three isostructural compounds relative to **1**, formulated as $[Co_{20}L1_{12}(OH)_{12}(H_2O)_4]\cdot 8X^-\cdot\chi$guest (X = ClO_4^-, PF_6^-, and $CF_3SO_3^-$ for **3**–**5**, respectively), were obtained (see Supporting Information). SCXRD revealed spontaneous resolution also occurred for **3**–**5**, similar to the case of **1** and **2**. However, no crystalline product formed when using NO_3^-, Cl^-, and Br^-, suggesting the anion effect should also be considered in assembling these metal–organic tetartoids into conglomerates.

A cubic cage ($[Co_8L3_6(H_2O)_6]\cdot 6BF_4^-\cdot\chi$guests) ($H_2L3$ = 1,3-bis[(5-methyl-1*H*-imidazol-4-yl)methyleneaminomethyl] benzene) can be assembled from 5-methyl-4-formylimidazole and *m*-xylylenediamine with $Co(BF_4)_2\cdot 6H_2O$ (Scheme 1).[16b] The only difference between L1 and L3 is the methyl position (2′ or 5′) located on imidazolyl. From the crystal structures, we found that the 2-methyl group resides inside the pentagonal window in the tetartoidal cage (Figure S11), while the 5-methyl group points out of the square window in the cubic cage (Figure S16). The small square window (H···H distance 3.843 Å, Figure S16) of the cubic cage does not allow additional methyl groups; therefore, larger pentagonal windows are formed in the self-assembly, giving a tetartoid. To prove the hypothesis, 2,5-dimethyl-4-formylimidazole and 4-formylimidazole were utilized to replace 2-methyl-4-formylimidazole, giving tetartoid **2** and cubic **6** ($[Co_8L4_6(NO_3)_6]\cdot\chi$guests, H_2L4 = 1,3-bis[(1*H*-imidazol-4-yl)-methyleneaminomethyl]benzene, Figure S17), respectively. These results indicate that 2-methyl substituent plays a structure-directing role to form the tetartoid due to steric effect, while 5-methyl has no preference in generating cubic or tetartoidal cages.

The positive cages in **1**–**5** are connected by anions to form diamond-like frameworks (Figure S4), which is similar to our reported supramolecular frameworks assembled from cubic cages and anions.[16b] Preliminary studies of gas adsorption property were performed by using cage **1** and **5**, which has higher yield. Their Brunauer–Emmett–Teller (BET) and Langmuir surface areas are calculated to be 145 and 447 m^2/g and 269 and 593 m^2/g, respectively, based on N_2 adsorption (77 K, Figure 4a), indicating permanent porosity. The big difference of porosity is probably due to different stability under vacuum conditions. PXRD measurements of the samples after gas adsorption showed that the crystallinity of **5** is better than that of **1** (Figure S19), indicating that **1** lost partial porosity. However, as shown in Figure 4b, their uptake abilities of CO_2 (**1** 58 and **5** 61 cm^3/g) and N_2 (**1** 3.6 and **5** 4.8 cm^3/g) at 273 K/100 kPa is similar. The capacity of gas adsorption for **1** and **5** is moderate, which is compared to some porous materials based on coordination cage.[18]

In conclusion, a series of chiral 20-nucleus coordination cages were assembled from 72 subcomponents. Co–imidazolate cages **1**–**5** represent the first examples of metal–organic tetartoid. Unusual spontaneous resolution of racemic tetartoidal cages into conglomerates of homochiral crystals are observed. Moreover, homochiral Δ and Λ cages can be induced by (D)- and (L)-menthol additives, providing a way to prepare homochiral cages by chiral induction. The formation of a tetartoidal cage is proven to be regulated by steric effect of the methyl substituents, giving a clue to assemble larger and emerging coordination cages by introducing bulky substituents on the ligand. Further applications on enantioselective separation and asymmetrical catalysis using these chiral cages are ongoing.

DOI: 10.1021/jacs.7b11285
J. Am. Chem. Soc. 2018, 140, 118–121

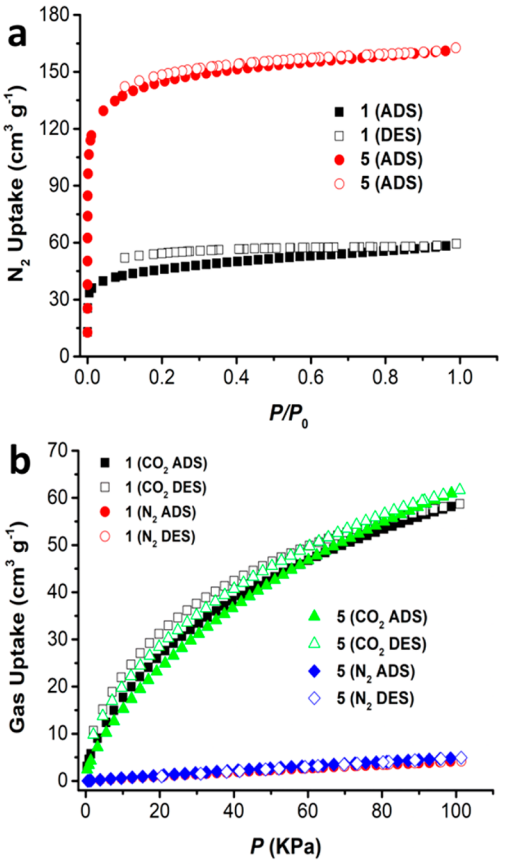

Figure 4. (a) N_2 at 77 K and (b) CO_2 and N_2 at 273 K adsorption/desorption isotherms of **1** and **5**.

■ ASSOCIATED CONTENT

Supporting Information

The Supporting Information is available free of charge on the ACS Publications website at DOI: 10.1021/jacs.7b11285.

Experimental section, physical measurements, crystallographic data (PDF)

CCDC nos. 1579418−1579428 (CIF)

■ AUTHOR INFORMATION

Corresponding Authors

*zhouxp@stu.edu.cn

*danli@jnu.edu.cn

ORCID

Xiao-Ping Zhou: 0000-0002-0351-7326

Dan Li: 0000-0002-4936-4599

Author Contributions

⊥D.L. and X.-Z.W. contributed equally to this work.

Notes

The authors declare no competing financial interest.

■ ACKNOWLEDGMENTS

Dedicated to Professor Chi-Ming Che on the occasion of his 60th birthday. This work was financially supported by the National Natural Science Foundation of China (Nos. 21731002, 91222202, and 21371113), the Guangdong Natural Science Funds for Distinguished Young Scholar (2014A030306042), the training program for Excellent Young College Teacher of Guangdong Province, and Jinan University.

■ REFERENCES

(1) (a) Khayat, R.; Tang, L.; Larson, E. T.; Lawrence, C. M.; Young, M.; Johnson, J. E. *Proc. Natl. Acad. Sci. U. S. A.* **2005**, *102*, 18944. (b) Chiu, W.; Rixon, F. J. *Virus Res.* **2001**, *82*, 9. (c) Zhou, Z. H.; Dougherty, M.; Jakana, J.; He, J.; Rixon, F. J.; Chiu, W. *Science* **2000**, *288*, 877. (d) Shi, B.; Jie, K.; Zhou, Y.; Zhou, J.; Xia, D.; Huang, F. *J. Am. Chem. Soc.* **2016**, *138*, 80. (e) Xia, D.; Wang, P.; Shi, B. *Org. Lett.* **2017**, *19*, 202. (f) Zhu, H.; Shangguan, L.; Xia, D.; Mondal, J. H.; Shi, B. *Nanoscale* **2017**, *9*, 8913.

(2) (a) Bilbeisi, R. A.; Ronson, T. K.; Nitschke, J. R. *Angew. Chem., Int. Ed.* **2013**, *52*, 9027. (b) Fujita, D.; Ueda, Y.; Sato, S.; Mizuno, N.; Kumasaka, T.; Fujita, M. *Nature* **2016**, *540*, 563. (c) Olenyuk, B.; Levin, M. D.; Whiteford, J. A.; Shield, J. E.; Stang, P. J. *J. Am. Chem. Soc.* **1999**, *121*, 10434.

(3) (a) Zarra, S.; Wood, D. M.; Roberts, D. A.; Nitschke, J. R. *Chem. Soc. Rev.* **2015**, *44*, 419. (b) Cook, T. R.; Stang, P. J. *Chem. Rev.* **2015**, *115*, 7001. (c) Smulders, M. M. J.; Riddell, I. A.; Browne, C.; Nitschke, J. R. *Chem. Soc. Rev.* **2013**, *42*, 1728. (d) Fujita, M.; Tominaga, M.; Hori, A.; Therrien, B. *Acc. Chem. Res.* **2005**, *38*, 369. (e) Seidel, S. R.; Stang, P. J. *Acc. Chem. Res.* **2002**, *35*, 972. (f) Byrne, K.; Zubair, M.; Zhu, N.; Zhou, X.-P.; Fox, D. S.; Zhang, H.; Twamley, B.; Lennox, M. J.; Düren, T.; Schmitt, W. *Nat. Commun.* **2017**, *8*, 15268. (g) Tranchemontagne, D. J.; Ni, Z.; O'Keeffe, M.; Yaghi, O. M. *Angew. Chem., Int. Ed.* **2008**, *47*, 5136. (h) Chen, L.-J.; Yang, H.-B.; Shionoya, M. *Chem. Soc. Rev.* **2017**, *46*, 2555. (i) Pan, M.; Wu, K.; Zhang, J.-H.; Su, C.-Y. *Coord. Chem. Rev.* **2017**, DOI: 10.1016/j.ccr.2017.10.031.

(4) (a) Brenner, W.; Ronson, T. K.; Nitschke, J. R. *J. Am. Chem. Soc.* **2017**, *139*, 75. (b) Garcia-Simon, C.; Garcia-Borras, M.; Gomez, L.; Parella, T.; Osuna, S.; Juanhuix, J.; Imaz, I.; Maspoch, D.; Costas, M.; Ribas, X. *Nat. Commun.* **2014**, *5*, 5557.

(5) (a) Kaphan, D. M.; Levin, M. D.; Bergman, R. G.; Raymond, K. N.; Toste, F. D. *Science* **2015**, *350*, 1235. (b) Cullen, W.; Misuraca, M. C.; Hunter, C. A.; Williams, N. H.; Ward, M. D. *Nat. Chem.* **2016**, *8*, 231. (c) Jing, X.; He, C.; Yang, Y.; Duan, C. *J. Am. Chem. Soc.* **2015**, *137*, 3967.

(6) Mal, P.; Breiner, B.; Rissanen, K.; Nitschke, J. R. *Science* **2009**, *324*, 1697.

(7) Zheng, Y.-R.; Suntharalingam, K.; Johnstone, T. C.; Lippard, S. J. *Chem. Sci.* **2015**, *6*, 1189.

(8) (a) Fujita, D.; Ueda, Y.; Sato, S.; Yokoyama, H.; Mizuno, N.; Kumasaka, T.; Fujita, M. *Chem.* **2016**, *1*, 91. (b) Sun, Q. F.; Iwasa, J.; Ogawa, D.; Ishido, Y.; Sato, S.; Ozeki, T.; Sei, Y.; Yamaguchi, K.; Fujita, M. *Science* **2010**, *328*, 1144.

(9) Kieffer, M.; Pilgrim, B. S.; Ronson, T. K.; Roberts, D. A.; Aleksanyan, M.; Nitschke, J. R. *J. Am. Chem. Soc.* **2016**, *138*, 6813.

(10) Zhou, X.-P.; Wu, Y.; Li, D. *J. Am. Chem. Soc.* **2013**, *135*, 16062.

(11) (a) Xuan, W.; Zhang, M.; Liu, Y.; Chen, Z.; Cui, Y. *J. Am. Chem. Soc.* **2012**, *134*, 6904. (b) Wu, K.; Li, K.; Hou, Y. J.; Pan, M.; Zhang, L. Y.; Chen, L.; Su, C. Y. *Nat. Commun.* **2016**, *7*, 10487.

(12) Fiedler, D.; Leung, D. H.; Bergman, R. G.; Raymond, K. N. *Acc. Chem. Res.* **2005**, *38*, 349.

(13) (a) Castilla, A. M.; Ramsay, W. J.; Nitschke, J. R. *Acc. Chem. Res.* **2014**, *47*, 2063. (b) Seeber, G.; Tiedemann, B. E. F.; Raymond, K. N. *Top. Curr. Chem.* **2006**, *265*, 147.

(14) Bonakdarzadeh, P.; Pan, F.; Kalenius, E.; Jurček, O.; Rissanen, K. *Angew. Chem., Int. Ed.* **2015**, *54*, 14890.

(15) Ronson, T. K.; Zarra, S.; Black, S. P.; Nitschke, J. R. *Chem. Commun.* **2013**, *49*, 2476.

(16) (a) Zhou, X.-P.; Liu, J.; Zhan, S.-Z.; Yang, J.-R.; Li, D.; Ng, K.-M.; Sun, R. W.-Y.; Che, C.-M. *J. Am. Chem. Soc.* **2012**, *134*, 8042. (b) Luo, D.; Zhou, X.-P.; Li, D. *Angew. Chem., Int. Ed.* **2015**, *54*, 6190.

(17) (a) Zhang, J.; Chen, S.; Wu, T.; Feng, P.; Bu, X. *J. Am. Chem. Soc.* **2008**, *130*, 12882. (b) Zhang, S.-Y.; Li, D.; Guo, D.; Zhang, H.; Shi, W.; Cheng, P.; Wojtas, L.; Zaworotko, M. J. *J. Am. Chem. Soc.* **2015**, *137*, 15406.

(18) (a) Dai, F.-R.; Wang, Z. *J. Am. Chem. Soc.* **2012**, *134*, 8002. (b) Wang, X.-S.; Chrzanowski, M.; Gao, W.-Y.; Wojtas, L.; Chen, Y.-S.; Zaworotko, M. J.; Ma, S. *Chem. Sci.* **2012**, *3*, 2823.

DOI: 10.1021/jacs.7b11285
J. Am. Chem. Soc. 2018, 140, 118−121